a second electrostatic analyzer (ESA-II). The field-free regions (FFR), located between the source and ESA-I (1st FFR) and between the magnet and ESA-II (3rd FFR), are equipped with standard collision cells. An Ion Tech saddle-field atom gun (Ion Tech, Middlesex, England) was used for producing 7 to 8 keV Ar atoms for FAB desorption in a commercially available Kratos FAB source.

For FAB-MS/MS experiments, an ion of interest was selected by using MS-I at a mass resolution of approximately 1000 (width at 10% height). Mass selected ion kinetic energy spectra (MIKES) were obtained by scanning MS-II. Twenty scans were averaged by using software written in this laboratory. CA experiments were done by activating the mass selected ion in the 3rd FFR by using a helium pressure that gave a 50% main beam suppression.

For MS/MS/MS experiments,[34] source-produced ions were activated in the first field free region. The fragment ion of interest was then transmitted to the third FFR by setting both the first ESA and the magnet at the appropriate values. The selected product ion was collisionally activated and the resultant fragment ions were analyzed by scanning the final electric sector.

(34) Burinsky, D. J.; Cooks, R. G.; Chess, E. K.; Gross, M. L. *Anal. Chem.* **1982**, *54*, 295-299.

For linked scans at constant B/E, source-produced ions were activated in the first FFR. ESA-I and the magnet were scanned at a constant B/E value determined by the ratio of the field strengths necessary to transmit precursor ions of the desired m/z ratio holding the accelerating potential (V) constant. Fragmentations occurring in the first FFR were observed in this way. The voltage applied to ESA-II followed that of ESA-I and the final detector (after ESA-II) was used.

Acknowledgment. Preliminary results were presented at the 36th ASMS Conference on Mass Spectrometry and Allied Topics, San Francisco, CA, 1988. This work was supported by the Midwest Center for Mass Spectrometry, a National Science Foundation Regional Instrumentation Facility (Grant No. CHE-8620177).

Registry No. Ala-Gly, 687-69-4; Gly-Ala, 3695-73-6; Leu-Gly, 686-50-0; Gly-Leu, 869-19-2; Ala-Ile, 29727-65-9; Ala-Leu, 3303-34-2; Leu-Ala, 7298-84-2; Gly-Ser, 7361-43-5; Gly-Phe, 3321-03-7; Hip-Phe, 744-59-2; Leu-Phe, 3063-05-6; Phe-Leu, 3303-55-7; Met-Phe, 14492-14-9; Phe-Met, 15080-84-9; Val-Lys, 22677-62-9; Lys-Val, 20556-11-0; Ala-His, 3253-17-6; His-Ala, 16874-75-2; His-Leu, 7763-65-7; His-Lys, 37700-85-9; Arg-Ala, 40968-45-4; Arg-Asp, 15706-88-4; Li^+, 17341-24-1.

Solvent Effects on the Interionic Structure of Ion Pairs. Electric Dipole Moments and Infrared Spectra of *N*-Allyl-*N*-ethyl-*N*-methylanilinium *p*-Toluenesulfonate Ion Pairs in a Series of Solvents[1]

M. Kohinoor Begum and Ernest Grunwald*

Contribution from the Chemistry Department, Brandeis University, Waltham, Massachusetts 02254. *Received December 15, 1989*

Abstract: Molar dielectric increments for *N*-allyl-*N*-ethyl-*N*-methylanilinium *p*-toluenesulfonate ion pairs (AEM^+Ts^-), measured at concentrations up to 3.5 mM, gave the following apparent dipole moments: 4.9 ± 0.2 D in benzene (ϵ 2.275); 8.1 ± 0.1 D in octanoic acid (HOct; ϵ 2.46); 7.0 ± 0.5 D in anisole (ϵ 4.33); 11.2 ± 0.3 D in chloroform (ϵ 4.72); 7.4 ± 0.5 D in chlorobenzene (ϵ 5.61); and 8.6 ± 0.2 D, both in 0.95 M HOct in benzene and in 1.00 M benzene in HOct. In non-hydrogen-bonding solvents ranging from benzene to dimethyl sulfoxide (ϵ 46.7), the S-O stretching absorption of Ts^- consisted of two nearly coalesced bands with maxima at 1220 ± 5 and 1198 ± 5 cm^{-1}. In formic, acetic, and octanoic acids this band shifted to 1145-1160 cm^{-1} owing to acceptance of a hydrogen bond by the SO_3^- group. Analysis of the carboxyl C=O stretching vibration in benzene indicated the formation of a 1:1 complex, formally AEM^+Ts^-·HOct, with an association constant of 280 ± 40 M^{-1}. In $CHCl_3$ the centroid of the S-O stretching absorption shifted little or not at all and gave no real evidence for hydrogen bonding. The marked variability of the ion-pair dipole moment is attributed at least in part to specific solvent-induced changes in the *average* interionic geometry, the ion pair being regarded as a solvent-dependent mixture of interionic structural isomers that differ in interionic tightness. Such changes are facilitated by the asymmetric structure of the AEM^+ cation, and the variation of tightness calls to mind the "intimate" and "solvent-separated" ion-pair isomers proposed[6] as intermediates in solvolysis.

In liquid solutions the interionic structure of an ion pair can be perturbed, relative to that in the gas phase, by physical and chemical solvation mechanisms.[2-8] In the chemical mechanisms, the cations and/or anions in the ion pairs form molecular complexes with solvent molecules, typically by donor-acceptor and/or hydrogen bonds.[2,4,6-8] In the physical mechanisms the solvent is represented as a dielectric continuum with specific properties or as a densely packed ensemble of specific molecules whose presence around the ion pair perturbs the interionic forces.[3,5] We shall take

(1) (a) This contribution is dedicated to the memory of Saul Winstein. (b) Work supported by the U.S. National Science Foundation.

(2) (a) Grunwald, E.; Highsmith, S.; I, T.-P. *Ions and Ion Pairs in Organic Reactions*; Szwarc, M., Ed.; Wiley-Interscience: New York, 1974; Vol. 2, Chapter 5. (b) Grunwald, E.; I, T.-P. *Pure Appl. Chem.* **1979**, *51*, 53; *J. Am. Chem. Soc.* **1974**, *96*, 2879.

(3) (a) Gilkerson, W. R. *J. Chem. Phys.* **1956**, *26*, 1199. (b) Fuoss, R. M. *J. Am. Chem. Soc.* **1958**, *80*, 5059. (c) Bottcher, C. F. J.; van Belle, O. C.; Bordewijk, P.; Rip, A. *Theory of Electric Polarization*, 2nd ed.; Elsevier: Amsterdam, 1973; Vol. 1.

(4) Davis, M. M. *Acid-Base Behavior in Aprotic Organic Solvents*; National Bureau of Standards Monograph 105; U.S. Government Printing Office: Washington, DC, 1968.

(5) Grunwald, E. *Anal. Chem.* **1954**, *26*, 1696.

(6) Winstein, S.; Clippinger, E.; Fainberg, A. H.; Robinson, G. C. *J. Am. Chem. Soc.* **1954**, *76*, 2597. Winstein, S.; Clippinger, E.; Fainberg, A. H.; Heck, R.; Robinson, G. C. *Ibid.* **1956**, *78*, 328.

(7) (a) Hogen-Esch, T. E.; Smid, J. *J. Am. Chem. Soc.* **1965**, *87*, 669. Roberts, R. C.; Szwarc, M. *Ibid.* **1965**, *87*, 5542. Carvajal, C.; Tolle, K. J.; Smid, J.; Szwarc, M. *Ibid.* **1965**, *87*, 5548. (b) Smid, J. *Ions and Ion Pairs in Organic Reactions*; Szwarc, M., Ed.; Wiley-Interscience: New York, 1972; Vol. 1, Chapter 3. Edgell, W. F. *Ibid.* Chapter 4. (c) Flora, H. B.; Gilkerson, W. R. *J. Phys. Chem.* **1976**, *80*, 679. (d) Onishi, S.; Farber, H.; Petrucci, S. *J. Phys. Chem.* **1980**, *84*, 2923.

(8) (a) de Boer, E.; Sommerdijk, J. L. *Ions and Ion Pairs in Organic Reactions*; Szwarc, M., Ed.; Wiley-Interscience: New York, 1972; Vol. 1, Chapters 7 and 8. (b) Sharp, J. H.; Symons, M. C. R. *Ibid.* Chapter 5. (c) Szwarc, M. *Ibid.* Appendix. (d) Greenberg, M. S.; Popov, A. I. *J. Solution Chem.* **1976**, *5*, 653. (e) Chuang, H.-J.; Soong, L.-L.; Leroi, G. E.; Popov, A. I. *Ibid.* **1989**, *18*, 759.

0002-7863/90/1512-5104$02.50/0

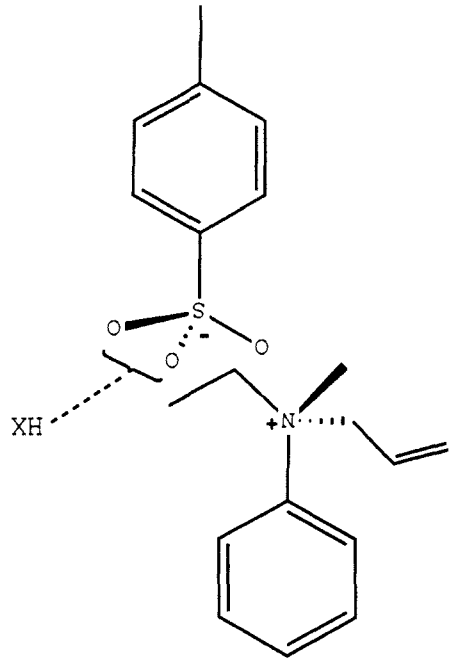

Figure 1. Structural formula of AEM^+Ts^-. The interionic geometry shown in the Figure is based on ref 9b. We believe that an H-bond donor, if present, would attach itself on the opposite side to the cation, either to one oxygen atom or, with a bifurcated hydrogen bond, to both oxygen atoms.

the latter point of view and focus on molecules and ions with irregular shapes.

Changes in interionic geometry can be detected by the changes they produce in a wide range of properties, including the reactivity of the ion pairs,[6] their electric dipole moments,[2] and their optical,[7] dielectric,[7d] and magnetic resonance absorptions.[8] In this paper we study the electric dipole moment and the infrared absorption in the region of the S–O stretching vibration for *N*-allyl-*N*-ethyl-*N*-methylanilinium *p*-toluenesulfonate (AEM^+Ts^-) ion pairs (Figure 1) in protic as well as aprotic solvents.

The AEM^+ cation, owing to its low symmetry (the nitrogen atom is chiral) and the presence of conformationally flexible *N*-ethyl and *N*-allyl groups, qualifies easily as an ion of complicated shape. The four substituents that emanate tetrahedrally from the nitrogen atom in a quaternary ammonium ion define four flexible cavities (Figure 2), each of which permits close approach to the cationic center of charge. Previous dipole moment measurements[9] for *N,N*-dimethyl-*N*-ethylanilinium *p*-toluenesulfonate ion pairs have shown that the Ts^- ion uses one cavity so as to bring one oxygen atom of the SO_3^- group into close approach (4–5 Å) to the N^+ center; the other cavities are next to solvent molecules. However, the lowest energy interionic geometry need not be the one with the best cation–anion interaction. Rather, the conformations of the cavity "walls" adjust so as to produce the best compromise between cation–anion and cation–solvent interactions. One expects that this compromise will vary with the nature of the solvent molecules. As a corollary, the distance between the ionic charge centers and the dipole moment of the ion pair will be solvent-dependent.

The preceding remarks apply to any quaternary ammonium ion, regardless of symmetry. When the four N substituents are chemically equivalent, the four cavities are also chemically equivalent. On the other hand, any nonequivalence among the N substituents will generate nonequivalence among the cavities and thus introduce an additional degree of freedom for solvent effects. For example, in the AEM^+ ion all four cavities are nonequivalent, as indicated in Figure 2. Accordingly, there exist

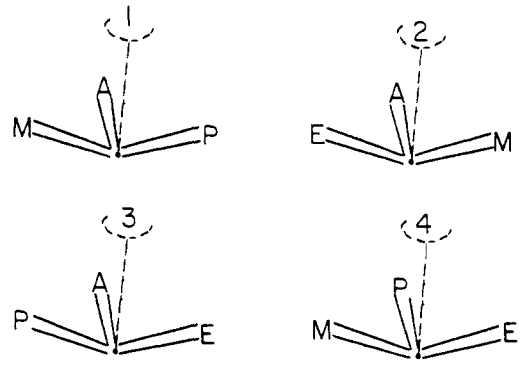

Figure 2. Schematic representation of the four nonequivalent cavities on the surface of the AEM^+ ion. The points at the junction of the bonded substituents represent N^+. A = allyl, E = ethyl, M = methyl, P = phenyl. The numerals represent the cavities.

four nonequivalent environments in which an SO_3–oxygen atom can be in close approach to the N^+ center, corresponding to four distinct interionic structural isomers. To find the most stable interionic geometry for the solvated ion pair, one now has the freedom not only of adjusting the conformations of the cavity walls but also of transferring the anion to a different cavity. Because of this added freedom, solvent effects on the dipole moment should be greater for asymmetric than for symmetric quaternary ammonium ion pairs. Our data, and data cited in the Discussion, support this view.

The *p*-toluenesulfonate ion (Ts^-) is more symmetrical than AEM^+, but nonetheless, it is a sensitive probe for physical solvation mechanisms and for hydrogen bonding. The electron distribution of Ts^- has an unusually large dipole moment superimposed on the ionic charge—a moment of 5.1 D, parallel to the 1,4-phenyl axis and pointing from SO_3^- to CH_3.[2a,9] A change in interionic geometry that causes a change in the angle between the phenyl axis and the line joining the ionic charge centers will, therefore, produce a relatively large change in the overall dipole moment of the ion pair. In addition, the SO_3^- group in the anion is a hydrogen-bond acceptor,[4,10] and hydrogen-bond donation by protic solvents can be probed by infrared spectroscopy.

Winstein and co-workers[6] inferred, from elegant kinetic studies, that in S_N1-type solvolysis there are two distinct ion-pair intermediates, which they described as "intimate" and "solvent-separated", respectively. Quaternary ammonium salts are often used as models for solvolysis intermediates and transition states, and in fact their thermodynamic solution properties resemble those of the transition states.[9c] The present results for AEM^+Ts^- thus are relevant to solvolysis. In particular, the experimental (i.e., rms average) molecular dipole moments of AEM^+Ts^- will be seen to vary greatly with the solvent, permitting the view that AEM^+Ts^- and related ion pairs, such as those considered by Winstein for solvolysis,[6] indeed consist of interionic isomers with marked differences in interionic tightness.

Results

Electric Dipole Moments. Dielectric constants of solutions of AEM^+Ts^- were measured at 25 °C in the following solvents: benzene, anisole, chlorobenzene, chloroform, octanoic acid, and two benzene–octanoic acid mixtures. Solute concentrations ranged up to 3.5 mM. Details of the audiofrequency measuring system have been reported previously.[9] Electrolytic dissociation was small, and corrections for the contribution of free ions to the solution capacitances[2b,11] were worth making only in anisole, chlorobenzene, and chloroform. These corrections, which were based on the theory of Onsager and Provencher,[12] required the estimation of two parameters and thereby nearly doubled the overall experimental

(9) (a) Dominey, L. A.; Comeford, L.; Chen, S. J.-H.; Grunwald, E. *J. Phys. Chem.* **1987**, *91*, 2211. (b) Comeford, L.; Grunwald, E.; Begum, M. K.; Pradhan, J. *Ibid.* **1990**, *94*, 2714. (c) Arnett, E. M.; Bentrude, W. G.; Burke, J. J.; Duggleby, P. McC. *J. Am. Chem. Soc.* **1965**, *87*, 1541.

(10) (a) Detoni, S.; Hadzi, D. *Proc. Colloq. Spectrosc. Int.*, 6th **1956**, p 601–8. (b) Simon, S.; Kriegsmann, H. *Chem. Ber.* **1956**, *89*, 1718.

(11) Highsmith, S.; Grunwald, E. *J. Phys. Chem.* **1974**, *78*, 1431.

(12) Onsager, L.; Provencher, S. W. *J. Am. Chem. Soc.* **1968**, *90*, 3134.

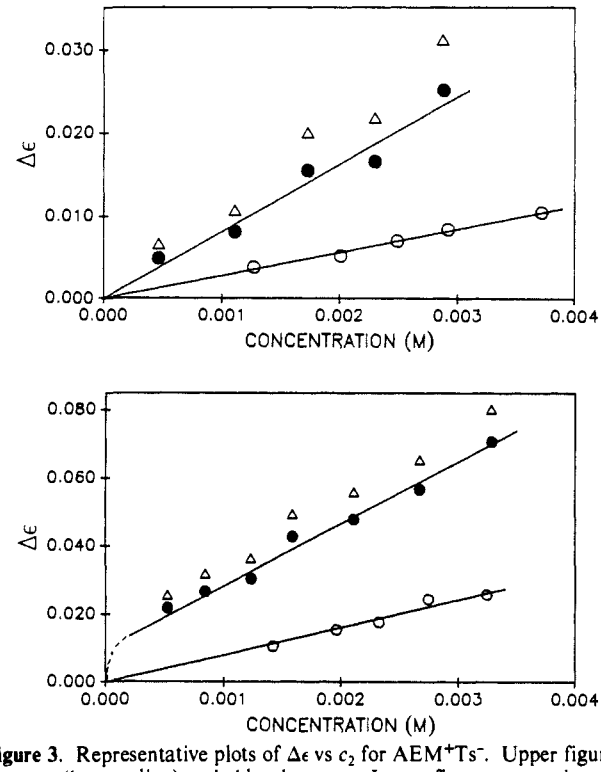

Figure 3. Representative plots of $\Delta\epsilon$ vs c_2 for AEM^+Ts^-. Upper figure: benzene (bottom line) and chlorobenzene. Lower figure: octanoic acid (bottom line) and chloroform. The triangles show the experimental results in chlorobenzene and chloroform prior to correction for the 90° out-of-phase component of the ionic conductivity. The least-squares straight lines (solid lines) fitting the data pass effectively through the origin, except in chloroform, where the intercept is 0.10.

error. Details are given in the Experimental Section.

Plots of dielectric constant ϵ vs the formal concentration c_2 of AEM^+Ts^- were straight lines within the experimental error in all solvents. Typical data are shown in Figure 3. The data for chlorobenzene and chloroform are shown both before and after a correction was applied for the contribution from free ions. The figure also reveals the striking variability of the slopes $d\epsilon/dc_2$ with the solvent.

The slopes $d\epsilon/dc_2$ were interpreted as molar dielectric increments due to the *ion pairs*. Apparent dipole moments $\mu_{2,app}$ of the ion pairs were then calculated by Onsager/Kirkwood theory. Specifics have been described previously.[13a] Results are listed in Table I. As might be expected from the variability of $d\epsilon/dc_2$, the apparent dipole moments vary considerably with the solvent.

A brief digression is now in order to define the physical significance of $\mu_{2,app}$. In nonassociating liquids, or whenever Onsager's theory is a good approximation, $\mu_{2,app}$ simply equals the intrinsic dipole moment μ_2 of the solute. If the solute interacts with solvent to produce a stoichiometric complex, or if it self-associates, a straightforward calculation beginning with $\mu_{2,app}$ will yield the dipole moment of the complex. In general, however, $\mu_{2,app}$ depends not only on the intrinsic dipole moment μ_2 but also on the rotational correlation of dipoles around solvent and solute molecules. In terms of Kirkwood's theory this dependence is expressed by eq 1,[13a] where g_1 and g_2 denote Kirkwood's rotational correlation

$$(\mu_{2,app})^2 = g_2\mu_2^2 + c_1\mu_1^2(dg_1/dc_2)_{c_2=0} \quad (1)$$

factors. Normally dg_1/dc_2 consists of two parts: a change in g_1 as some solvent molecules enter the solvation shell of the solute and a further change in g_1—now in the bulk solvent—as the molecular network of the bulk solvent is perturbed by the introduction and solvation of the solute. The first part is calculated with use of the same model that applies to g_2. The second part is the solute-induced medium effect.[13b] However, for the present solvents the solute-induced medium effect may be neglected, for the following reasons: (1) Benzene is nonpolar. (2) Anisole, chlorobenzene, and chloroform are normal liquids with negligible dipole correlations: $g_1 \approx 1$ on the basis of dielectric constants of the pure liquids.[14] (3) Octanoic acid is largely associated to a nonpolar hydrogen-bonded dimer. Previous work has shown, however, that the apparent dipole moments of non-hydrogen-bonding solutes ($g_2 = 1$) in octanoic acid are equal to their intrinsic dipole moments.[13c] This implies that $dg_1/dc_2 \approx 0$ and that solute-induced medium effects thus are negligible. Presumably the nonpolar dimeric structure of liquid octanoic acid is too stable to be changed by the mere presence of an inert solute. To confirm this conclusion, we made new measurements, using diphenylsulfone as a highly polar, partly aromatic model compound. The result for the apparent dipole moment in octanoic acid is 5.3 ± 0.3 D, which is statistically indistinguishable from the intrinsic dipole moment of 5.0 ± 0.1 D measured for diphenylsulfone in benzene.[15] Furthermore, the infrared wavenumbers in the S–O stretching region of diphenylsulfone in benzene do not shift when 0.95 M octanoic acid is added, showing that hydrogen bonding is unimportant.

Table I. Apparent Dipole Moments of *N*-Allyl-*N*-ethyl-*N*-methylanilinium *p*-Toluenesulfonate at 25 °C

solvent	ϵ_0	$d\epsilon/dc_2$[a]	$\mu_{2,app}$ (D)[b]
benzene (B)	2.275	2.8 ± 0.2	4.9 ± 0.2
octanoic acid (HOct)	2.46	8.0 ± 0.2	8.3 ± 0.1
0.95 M HOct in B	2.29_6	8.6 ± 0.3	8.6 ± 0.2
1.00 M B in HOct	2.44	8.7 ± 0.3	8.6 ± 0.2
anisole[c]	4.33	7.2 ± 0.8	7.0 ± 0.5
chloroform[c,d]	4.72	18.2 ± 1.0	11.2 ± 0.3
chlorobenzene[c]	5.61	8.1 ± 1.0	7.4 ± 0.5

[a] Molar dielectric increment. [b] V_2 = 296.2 mL/mol; R_2 = 100.2 mL/mol. [c] Results have been corrected for the contribution by free ions to the capacitance with use of the following equivalent conductances: 43 (anisole), 70 (chloroform), 50 (chlorobenzene). For $(a - {}^1/_2)$, we used a middle value of 0.5. The error estimates in the table include the effects of uncertainty in these parameters. [d] The plot of ϵ vs c_2 has an intercept of 0.010; see Figure 3.

Accordingly, the solvent effects on $\mu_{2,app}$ described in Table I result either from changes in the average interionic geometry leading to changes in μ_2 or from dipole orientation effects in the solvation shells leading to consistent changes in g_2 and dg_1/dc_2. To learn about the latter, we shall now report infrared studies of hydrogen bonding by the ion pairs.

Infrared Spectra in the Region of the S–O Stretching Vibration. To obtain evidence for hydrogen bonding, we examined the S–O stretching vibrations of the SO_3^- group in the infrared.[9a,10] In the range of interest, 900–1300 cm^{-1}, there is a diversity of solvent absorptions, some of which are strong. To preserve useable transmittancy in most of this region, we used short optical paths, either 0.1-mm cells or cells with still shorter optical paths of unknown thickness produced by placing films of the substrate liquids between NaCl plates.

Solution and solvent spectra were stored in a computer, and difference spectra (of optical density) as well as subtraction spectra (of transmittance) were computed. Both spectra gave the same fingerprints of the solute absorption, but the subtraction spectra tended to be clearer because the instrumental noise was more uniform.

Representative subtraction spectra between 900 and 1300 cm^{-1} in a series of non-hydrogen-bonding solvents are shown in Figure 4.

The concentrations of AEM^+Ts^- are mostly dilute, being limited by the solubilities. According to prior assignments,[9a,10,16-18] be-

(13) (a) Grunwald, E.; Pan, K.-C. *J. Phys. Chem.* **1976**, *80*, 2929. (b) Grunwald, E.; Anderson, S. P.; Effio, A.; Gould, S. E.; Pan, K.-C. *Ibid.* **1976**, *80*, 2935. (c) I, T.-P.; Grunwald, E. *J. Am. Chem. Soc.* **1976**, *98*, 1351.

(14) Riddick, J. A.; Bunger, W. B.; *Organic Solvents*, 3rd ed.; Wiley-Interscience: New York, 1970.

(15) McClellan, A. L. *Tables of Experimental Dipole Moments*; W. H. Freeman and Co.: New York, 1963; Vol. 1; Rahara Enterprises: 1974; Vol. 2; Rahara Enterprises: 1989; Vol. 3.

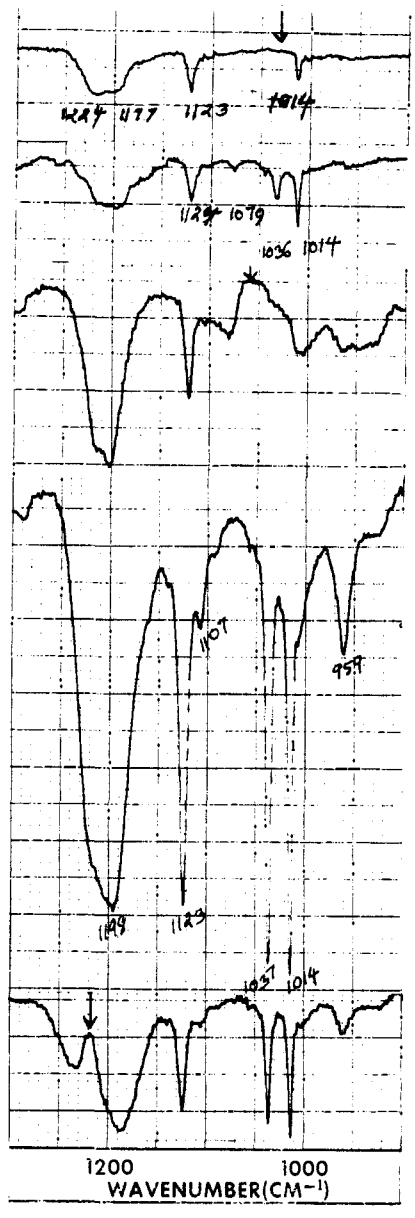

Figure 4. Representative subtraction spectra for AEM^+Ts^- between 900 and 1300 cm^{-1} in (top to bottom) benzene, anisole, dimethyl sulfoxide, dichloromethane, and chloroform. Values of ν_{max} for very strong solvent absorption are indicated by vertical lines.

tween 900 and 1300 cm^{-1}, one expects to see S–O stretching absorption and, perhaps weakly, phenyl absorption. Crystalline metallic benzenesulfonate salts[10a] and *N*-trimethylanilinium para-substituted benzenesulfonate salts in aprotic solvents[9a] show two overlapping absorption bands near 1200 cm^{-1}, which have been assigned to S–O stretching vibrations. Detoni and Hadzi[10a] also interpreted a weaker band at 1140 cm^{-1} as an S–O stretch. According to Colthup,[18] monosubstituted benzenes show phenyl absorption at 1150 ± 15, 1080 ± 20, and 1030 ± 15 cm^{-1}. Disubstituted benzenes show phenyl absorption at 1200 ± 20, 1110 ± 15, 1050 ± 15, 1010 ± 15, and 980 ± 15 cm^{-1}. According to Bellamy,[16] these phenyl absorptions may be weak and thus may not be visible under our conditions.

In our control experiments in several solvents, the spectra obtained for K^+Ts^- and Li^+Ts^- between 900 and 1300 cm^{-1} were qualitatively identical with those of AEM^+Ts^-, showing that absorption by the AEM^+ cation is not detectable under our conditions. Absorption between 900 and 1300 cm^{-1} thus is interpreted as phenyl or S–O stretching absorption due to the Ts^- anion. The two kinds of absorption can be distinguished experimentally because the phenyl frequencies are expected to be nearly independent of the solvent, while the S–O stretching frequencies will decrease when the SO_3^- group accepts hydrogen bonds. On that basis, the bands in our spectra at 1125, 1037, 1013, and 960 cm^{-1} (±2 cm^{-1}) are phenyl absorptions of the Ts^- ion. These wavenumbers agree with four of Colthup's five correlations[18] for 1,4-disubstituted benzenes. (We did not see the fifth, which is expected near 1200 cm^{-1} and is in the region of the S–O stretching vibration.) In particular, the bands at 1125 and 1013 cm^{-1} appear in all solvents. The band at 1037 cm^{-1} appears in all solvents except benzene and tetrahydrofuran (THF), where it is masked by very strong solvent absorption (benzene at 1032 cm^{-1}, THF at 1065 cm^{-1}; our solvent control spectra were practically opaque at 1037 cm^{-1}). The band at 960 cm^{-1} is weaker but is visible in most solvents, protic as well as aprotic.

As expected, the S–O stretching absorption is found near 1200 cm^{-1} in all non-hydrogen-bonding solvents, including benzene, THF, dichloromethane, anisole, chlorobenzene, dimethyl sulfoxide, and probably $CHCl_3$ (see below). This absorption is relatively strong and broad and consists of two nearly coalesced bands centered at 1220 ± 5 and at 1198 ± 5 cm^{-1}, respectively (Figure 4). In dimethyl sulfoxide, where AEM^+Ts^- is largely dissociated to free ions (ϵ 46.7), the absorption is slightly narrower. The KBr pellet spectrum of AEM^+Ts^- shows strong absorption centered at 1200 cm^{-1}, consisting of at least two unresolved bands, in agreement with the aprotic solution spectra.

In $CHCl_3$, the absorption seems to be well resolved into two components with maxima at 1235 and 1188 cm^{-1}. We believe, however, that this is an artifact resulting from strong $CHCl_3$ solvent absorption centered at 1217 cm^{-1} and corresponding compression of the subtraction spectrum owing to compression of the transmittance scale at low transmittances. Note in particular that the minimum in the subtraction spectrum at 1218 cm^{-1} agrees very well with the absorption maximum of $CHCl_3$ at 1217 cm^{-1}. In any case, the centroid of the S–O stretching absorption in $CHCl_3$ is shifted at most by −8 cm^{-1} relative to its average position in the other aprotic solvents.

Unambiguous frequency shifts due to hydrogen bonding to the SO_3^- group were observed in carboxylic acid media. The effect of successive additions of octanoic acid (HOct) to solutions of AEM^+Ts^- in benzene is shown in Figure 5. (Compare with the top spectrum in Figure 4.) The figure shows the progressive diminution of the original bands near 1200 cm^{-1} and the growing-in of a new band around 1158 cm^{-1} as octanoic acid is added. In pure octanoic acid, the absorption near 1200 cm^{-1} has disappeared and the absorption correlated with the new band occurs at ~1145 cm^{-1}. In addition, there is a second new band, broad and relatively weak, centered near 1090 cm^{-1}.

Figure 6 shows the subtraction spectra of potassium *p*-toluenesulfonate in the deciformal range in octanoic, acetic, and formic acids. In octanoic and acetic acids, solution conductivities are small, while in formic acid (ϵ 58), conductivity measurements indicate that KTs consists predominantly of free ions. Comparison of Figures 6 and 5 shows that the octanoic acid spectrum of KTs is very similar to that of AEM^+Ts^-. Both spectra show a hydrogen-bonded S–O stretching band near 1145 cm^{-1} and a broad weak band near 1090 cm^{-1}. In acetic and formic acids the hydrogen-bonded S–O stretching band becomes centered near 1160 cm^{-1}. The band near 1090 cm^{-1} is present in acetic acid but seems to have disappeared in formic acid, where ionic dissociation is almost complete.

In their IR study of crystalline metallic benzenesulfonate salts, Detoni and Hadzi[10a] also observed a band at 1140 cm^{-1}, which they assigned to an S–O stretching motion. While our IR spectra in aprotic solvents show no counterpart to that band, our spectra in the carboxylic acid solvents do. Perhaps their 1140-cm^{-1} band is due to the presence of a few hydrated crystals in their sample. In a previous paper from this laboratory,[10a] a band at 1122 cm^{-1} that corresponds to the phenyl vibration at 1125 cm^{-1} was mis-

(16) Bellamy, L. J. *The Infrared Spectra of Complex Molecules*, 3rd ed.; Chapman and Hall: London, 1975; Vol. 1.
(17) Avram, M.; Mateescu, Gh. *Infrared Spectroscopy, English Translation* Wiley-Interscience: New York, 1972.
(18) Colthup, N. B. *J. Opt. Soc. Am.* **1950**, *40*, 397.

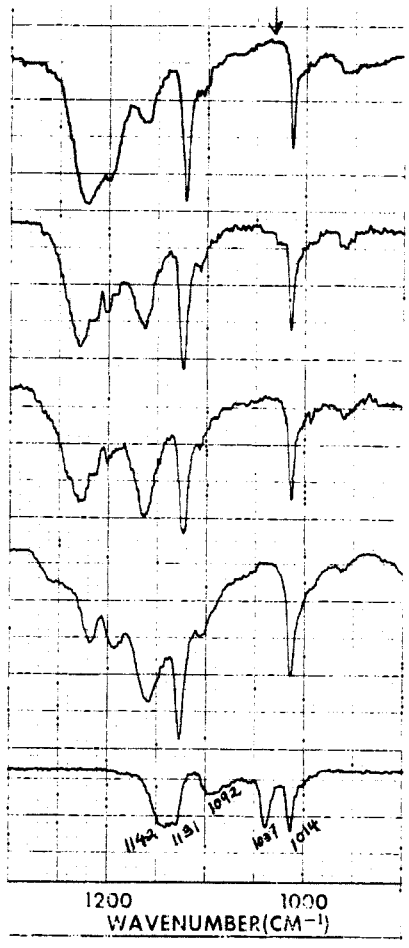

Figure 5. Representative subtraction spectra for (0.04 M AEM^+Ts^- + m M octanoic acid) in benzene vs m M octanoic acid in benzene. Top to bottom: m = 0.02, 0.05, 0.11, and 0.95* M, and pure octanoic acid*. (*In these solvents the concentration of AEM^+Ts^- is in the decimolar range.) The spectrum of AEM^+Ts^- in pure benzene is shown at the top in Figure 4.

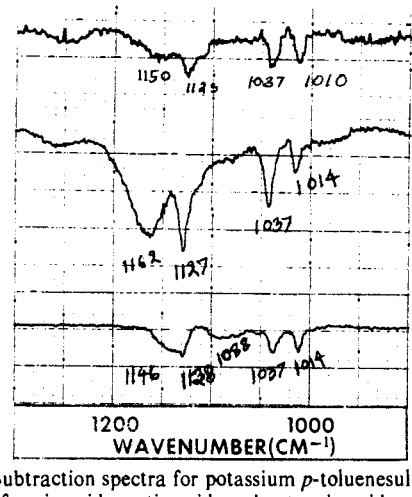

Figure 6. Subtraction spectra for potassium p-toluenesulfonate in (top to bottom) formic acid, acetic acid, and octanoic acid.

takenly identified as a phenyl–sulfur stretch. We are now pleased to correct that assignment.

In summary, in the aprotic solvents the S–O stretching absorption appears as a nearly coalesced doublet near 1200 cm^{-1}, which provides a fingerprint for the non-hydrogen-bonded SO_3^- group. In the carboxylic acids, this absorption disappears and a broad new band appears, with a maximum at 1145–1160 cm^{-1}. As octanoic acid is added to benzene, the new band grows in, but even at 0.95 M octanoic acid some non-hydrogen-bonded S–O stretching absorption remains. The absence of such absorption

Table II. Hydrogen Bonding of Octanoic Acid with AEM^+Ts^- in Benzene at 25 °C and Fit of Equation 3 to Absorbance Data at 1714 cm^{-1}

formal concn (M)		equil concn (M)		
c_{HOct}	$c_{AEM^+Ts^-}$	[HOct][a]	$[\sim\sim SO_3^-\cdot HOct]$	K_3 (M^{-1})
0.0186	0.0226	0.0020	0.0086	310
0.0277	0.0421	0.0022	0.0154	260
0.0402	0.0435	0.0030	0.0197	280
0.0473	0.0401	0.0033	0.0218	360
0.0699	0.0422	0.0045	0.0249	320
0.0918	0.0424	0.0055	0.0251	260
0.1121	0.0422	0.0064	0.0241	210
			ave	280 ± 40

[a] Molar concentration of monomer.

in pure octanoic acid solvent thus suggests that hydrogen bonding in that medium is practically complete. In chloroform the S–O stretching absorption is perturbed by strong $CHCl_3$ solvent absorption, but the centroid shifts little or not at all and provides no real evidence for hydrogen bonding.

Hydrogen Bonding between AEM^+Ts^- and Octanoic Acid in Benzene. Because of the marked increase in the apparent dipole moment of AEM^+Ts^- when 0.95 M octanoic acid is added to benzene (Table I), we decided to study the solution chemistry in greater detail. Two equilibria were of interest: the self-association of octanoic acid and its hydrogen bonding to AEM^+Ts^-. The self-association of octanoic acid (2) has not been measured pre-

$$2HOct \rightleftarrows HOct_2 \qquad K_2 = [HOct_2]/[HOct]^2 \qquad (2)$$

viously, but data for other carboxylic acids[4] indicate that the equilibrium constant K_2 would be of magnitude 500–1000 M^{-1} in benzene. To obtain an experimental value, we measured optical densities at the peak of the O–H stretching band of octanoic acid monomer (3485 ± 5 cm^{-1} in benzene), at 0.0015–0.0066 volume formal acid concentrations. (The O–H stretch of the dimer is at 3220 ± 10 cm^{-1} in benzene.) The "best value" obtained for K_2 is 1000 M^{-1} (+500, −300) in benzene at 25 °C. By using that value, molar extinction coefficients are 300 for the monomer and ≈100 for the dimer.

To determine complex formation between AEM^+Ts^- and octanoic acid, we examined the C=O stretching absorption of octanoic acid in the region 1700–1800 cm^{-1}. Band wavenumbers were assigned as follows: for HOct monomer, at 1755 ± 5 cm^{-1}; for $HOct_2$ dimer, at 1714 ± 2 cm^{-1}; for the complex between HOct and AEM^+Ts^-, at 1735 ± 5 cm^{-1}. Absorption by liquid benzene at these wavenumbers is very slight.

The monomer absorption at 1755 cm^{-1} was too weak to be useful, but the bands at 1735 and 1714 cm^{-1} were analyzed after small corrections were applied for band overlap. For both bands the data favored a 1:1 stoichiometry by formula weight.

Before proceeding further, a brief discussion of stoichiometric issues is now in order. As shown in Table II, the AEM^+Ts^- formal concentrations are 1 order of magnitude greater than those in the dielectric measurements. Even though the absence of curvature in the dielectric plot of the latter (Figure 3, benzene) is consistent with the presence of simple ion pairs, self-association to double ion pairs[19] and/or oligomeric aggregates[20] now becomes a distinct possibility and would generate nonequivalent sets of SO_3^- groups. As hydrogen bonding proceeds, the number of nonequivalent sets would increase further. In principle, each of the nonequivalent sets has a specific hydrogen-bond acceptor reactivity, and a rigorous formulation of the multiple coupled equilibria is complicated. In practice, however, the acceptor reactivities may be sufficiently equal so that the hydrogen bonding may be formulated simply as in (3), where $\sim\sim SO_3^-$ denotes any non-hydrogen-bonded SO_3^-

(19) (a) Geddes, J. A.; Kraus, C. A. *Trans. Faraday Soc.* **1936**, *32*, 585. (b) Fuoss, R. M. *J. Am. Chem. Soc.* **1934**, *56*, 1031. (c) Fuoss, R. M.; Kraus, C. A. *Ibid.* **1935**, *57*, 1.

(20) (a) Kraus, C. A.; Vingee, R. A. *J. Am. Chem. Soc.* **1934**, *56*, 511. (b) Batson, F. M.; Kraus, C. A. *Ibid.* **1934**, *56*, 2017. (c) Rothrock, D. A.; Kraus, C. A. *Ibid.* **1937**, *59*, 1699.

$$\sim\sim SO_3^- + HOct \rightleftarrows \sim\sim SO_3^-\cdot HOct \qquad K_3 = [\sim\sim SO_3^-\cdot HOct]/[HOct][\sim\sim SO_3^-] \quad (3)$$

group, and $\sim\sim SO_3^-\cdot HOct$ denotes any SO_3^- group that is hydrogen-bonded to octanoic acid monomer. Results based on absorbances measured at 1714 cm^{-1} are listed in Table II. The final column shows that the equilibrium formulated in (3) fits rather well. With use of a value of 1000 M^{-1} for K_2, the average K_3 for hydrogen bonding is 280 ± 40 M^{-1}.

Although the formulation of eq 3 is an approximation when the ion pairs self-associate, it becomes exact when such processes are absent. In that case, K_3 is a genuine constant for the simple equilibrium HOct + AEM^+Ts^- ⇄ $AEM^+Ts^-\cdot HOct$. On the other hand, if there were a variety of ion-pair aggregates, K_3 would decrease with increasing octanoic acid concentration (at constant $c_{AEM^+Ts^-}$) because the most reactive SO_3^- groups would tend to accept hydrogen bonds first. Within the accuracy of the data, no such trend is visible in Table II. Moreover, extrapolation to 0.95 M octanoic acid predicts that 14% of the SO_3^- groups still remain non-hydrogen-bonded, so there is no conflict with the existence of non-hydrogen-bonded S–O stretching absorption at that concentration in Figure 5.

The solubility of AEM^+Ts^- is increased strongly by the presence of octanoic acid. Thus, there is little doubt that the magnitude deduced for K_3 from the infrared data is correct, even though an association constant of 280 M^{-1} would seem rather high for hydrogen bonding if the ligands were nonionic. As indicated in Figure 1, the hydrogen bond might be an ordinary hydrogen bond to one of the "free" oxygen atoms ("free" meaning relatively distant from the N^+ center) or a bifurcated hydrogen bond involving both of those oxygen atoms.

Experimental Section

Materials. *N*-Allyl-*N*-ethyl-*N*-methylanilinium *p*-toluenesulfonate was synthesized by a procedure developed in this laboratory by N. V. Amin.[21] In the first step, *N*-methylaniline was treated in acetic acid with sodium borohydride.[22] The resulting *N*-ethyl-*N*-methylaniline was then quaternarized with allyl iodide and the iodide salt metathesized to the *p*-toluenesulfonate salt with silver *p*-toluenesulfonate. The recrystallized substrate, mp 85–86 °C, was stored in a vacuum desiccator. IR band maxima up to 1300 cm^{-1} in aprotic solvents and their assignments are as follows: 561 (SO_3 deformation), 684 (phenyl–S stretch), 762 (CH out-of-plane deformation of cation), 817 (CH out-of-plane deformation of anion), 960, 1013, 1037, 1125 (phenyl vibrations of anion), 1220, 1198 cm^{-1} (SO_3 stretch).

Solvents of Gold Label quality were further purified and dried (if necessary) by accepted procedures[9,14] and freshly distilled prior to use. Stock solutions were prepared in 25–50-mL batches by stirring weighed amounts of substrate and solvent on a warm hot plate, with precautions to exclude atmospheric moisture. After appropriate dilution, the solutions were introduced by syringe into the septum-stoppered dielectric cells.

Dielectric measurements were made at 20 kHz, with a calibrated General Radio audiofrequency bridge and a stainless-steel concentric spherical cell. Cell design and cleaning procedures have been described in a recent publication.[9b] Both capacitance and conductance were measured.

On the basis of measured conductances, conductivities were less than 10^{-11} $[\Omega\cdot cm]^{-1}$ for the pure solvents and for solutions in benzene, octanoic acid, and their mixtures. Conductivities ($[\Omega\cdot cm]^{-1}$) were (0.2–1) × 10^{-8} in anisole, (1.2–5) × 10^{-8} in chlorobenzene, and (2–10) × 10^{-8} in chloroform. The corresponding ionic strengths (i.e., concentrations of dissociated electrolyte) were 0.05–0.3 μM in anisole, 0.25–0.9 μM in chlorobenzene, and 0.3–1.5 μM in chloroform.

Experimental values of the capacitance were corrected for the 90° out-of-phase component of the ionic conductances by Highsmith and Grunwald's equations 1–6.[11] The calculation involved two parameters: the equivalent conductivity of the dissociated ions, which was estimated by applying Walden's rule to known values for quaternary anilinium *p*-toluenesulfonates in aprotic solvents, and a kinetic parameter ($a - {}^1/_2$) whose value is the ratio of the actual to the diffusion-controlled rate constant for free-ion recombination.[11,12] The physically possible range of ($a - {}^1/_2$) is 0–1; we used a middle value of 0.5.

Infrared spectra were recorded on a Perkin-Elmer Model 683 grating infrared spectrophotometer. The optical cells consisted of NaCl plates separated by nominally 0.1- or 0.5-mm Teflon spacers or without spacers and separated by a thin layer of the substrate liquid.

Discussion

The apparent dipole moments in Table I range from 5 D in benzene to 11 D in chloroform. Most values are near 8 D. In benzene, the ion pairs of some quaternary ammonium salts are known on the basis of freezing point data[19a,20] to exist measurably in equilibrium with double and higher order ion pairs at millimolar concentrations, that is, in our experimental range. In such cases the plot of ϵ vs c_2 shows negative curvature, because the ion-pair complexes are relatively nonpolar.[19,20,23,24] Other quaternary ammonium salts, which give straight-line plots at millimolar concentrations, consist of simple ion pairs.[19,20] Our dielectric data, shown in Figure 3, are best fit by a least-squares straight line passing through the origin and thus indicate simple ion pairs. Similarly, the data for K_3 in Table II at 10-fold higher salt concentrations are consistent with a single set of SO_3^- groups and thus again indicate simple ion pairs.

At the 11-D end of the range, in chloroform, the apparent dipole moment may contain a direct contribution from hydrogen bonding with $CHCl_3$, but we believe that any such contribution would be small. The S–O stretching band of Ts^- in chloroform shows only a small frequency shift, at most −8 cm^{-1} as compared to −50 cm^{-1} in octanoic acid, suggesting that hydrogen bonds with $CHCl_3$, if present, are weak. Moreover, the molecular dipole moment of $CHCl_3$ is small, 1.18 D in benzene,[15] and if hydrogen bonds with $CHCl_3$ are formed, they will not be very effective at raising the apparent dipole moment of the ion pair. We believe, therefore, that at least part of the elevation of the dipole moment in chloroform comes from a change in the average interionic structure of the ion pairs.

In 0.95 M octanoic acid in benzene, the principal ion-pair species is the 1:1 complex, $AEM^+Ts^-\cdot HOct$. When the apparent dipole moment is interpreted on that basis, the intrinsic dipole moment of $AEM^+Ts^-\cdot HOct$ becomes 8.7 D. The dipole moment of AEM^+Ts^- in benzene is 4.9 D, that of octanoic acid monomer is 3.9 D for the trans COOH conformation, and 1.4 D for the cis COOH conformation.[2b] If the 1:1 complex was formed without change in polar character in the ligands, the maximum value for the dipole moment of $AEM^+Ts^-\cdot HOct$ would be 4.9 + 3.9 D, or 8.8 D, which is close to the experimental result. This maximum, however, describes an implausible model in which the hydrogen bond is nearly inflexible, with the AEM^+Ts^- dipole and the trans carboxyl dipole being parallel. We prefer instead a model in which the hydrogen bond is flexible and the AEM^+Ts^- ion pair becomes more polar in the complex. One mechanism by which this might happen is that the centroid of charge in the SO_3^- group, which is polarized away from the 3-fold axis toward N^+ in AEM^+Ts^-, moves a short distance toward the hydrogen-bond acceptor site in $AEM^+Ts^-\cdot HOct$. (See Figure 1.)

Taken as a whole, our results demonstrate that the apparent dipole moment, and hence the average interionic geometry, of an ion pair can vary with the solvent even when molecular complex formation with solvent molecules is weak or negligible. A useful theory is that ion pairs are mixtures of interionic isomers whose equilibrium ratios and individual interionic geometries vary with the solvent. Given the spread from the highest to the lowest of the apparent dipole moments, these mixtures may include isomers differing in interionic tightness, such as the "intimate" and "solvent-separated" ion pairs proposed by Winstein and his coworkers[6] to account for kinetic, steric, and product results in solvolysis.

We believe that the present results for AEM^+Ts^- represent the largest medium effects ever reported for the apparent dipole moment of a quaternary ammonium ion pair. This may be because AEM^+ is unsymmetrical while the previous studies all involved symmetrical tetraalkylammonium ions.[2a] Extensive data exist for

(21) Amin, N. V. In preparation.
(22) Marchini, P.; Liso, G.; Reho, A.; Liberatore, F.; Moracci, F. M. *J. Org. Chem.* **1975**, *40*, 3453.
(23) Bauge, K.; Smith, J. W. *J. Chem. Soc.* **1964**, 4244.
(24) I, T.-P.; Grunwald, E. *J. Am. Chem. Soc.* **1974**, *96*, 2387.

tetra-*n*-butylammonium picrate in a series of non-hydrogen-bonding solvents ranging in dielectric constant from 2.2 to 6.0.[25,26] The apparent dipole moments in this series range from 13.8 to 16.8 D and vary in a random manner with the dielectric constant. Less extensive solvent effects are known for tetra-*n*-butylammonium bromide and for tetraisoamylammonium nitrate and iodide.[25,27] Here the changes in the apparent dipole moment are 1.6, 0.6, and 2.5 D, respectively. Dielectric relaxation has been studied for tetra-*n*-butylammonium perchlorate in a number of aprotic and hydrogen-bonding solvents whose dielectric constants range from 3.3 to 20.7D.[28] Measurements at the lowest frequencies in this study[28] indicate that molar dielectric increments vary with the solvent, but the frequencies of the measurements were too high for dipole moments to be reported.

In conclusion, our results for AEM^+Ts^- demonstrate that the average electric dipole moments of quaternary ammonium ion pairs can vary considerably with the solvent, not only because of hydrogen bonding to the anion in appropriate solvents but because of changes in the average interionic geometry. Such changes can arise, first, because the formal ion-pair species may in fact be a mixture of interionic isomers whose equilibrium ratios vary with the solvent and, second, because the interionic geometries of the individual ion-pair isomers may vary with the solvent.

(25) Gilkerson, W. R.; Srivastava, K. K. *J. Phys. Chem.* **1960**, *64*, 1485.
(26) Richardson, E. A.; Stern, K. H. *J. Am. Chem. Soc.* **1960**, *82*, 1296.
(27) Grunwald, E.; Effio, A. *J. Solution Chem.* **1973**, *2*, 373, 393.
(28) Sigvartsen, T.; Gestblom, B.; Noreland, E.; Songstad, J. *Acta Chem. Scand.* **1989**, *43*, 103.

Collisional Activation of Distonic Radical Cations and Their Conventional Isomers in Quadrupole Tandem Mass Spectrometry

Vicki H. Wysocki*,† and Hilkka I. Kenttämaa*

Contribution from the Department of Chemistry, Purdue University, West Lafayette, Indiana 47907-3699. *Received September 18, 1989*

Abstract: Competition between collision-activated isomerization and fragmentation of the distonic radical cations $^{\bullet}CH_2(CH_2)_nOH_2^+$ (n = 0–2) and their conventional counterparts ($CH_3(CH_2)_nOH^{\bullet+}$, n = 0–2), was examined under different experimental conditions in a triple quadrupole mass spectrometer and in a Paul-type quadrupole ion trap. All the above pairs of isomers give structurally characteristic fragmentation products upon low-energy (eV) collisional activation under single- and multiple-collision conditions in the triple quadrupole instrument. Fast direct bond cleavages dominate the fragmentation. Thus, abundant even-electron ionic fragments are obtained for the conventional ions, while the distonic isomers yield predominantly odd-electron ionic fragments. Further, the results suggest that the barrier between the ions $CH_3CH_2CH_2OH^{\bullet+}$ and $^{\bullet}CH_2CH_2CH_2OH_2^+$ is significantly lower than the barriers associated with the shorter chain homologues (n = 0 or 1). This is consistent with findings reported recently for the nitrogen analogues. The quadrupole ion trap yielded collision-activated dissociation spectra that were indicative of distinct structures *only* for the isomers $CH_3CH_2OH^{\bullet+}$ and $^{\bullet}CH_2CH_2OH_2^+$. This is explained on the basis of the observation that the light helium target used for collisional activation in the ion trap makes fragmentation pathways with high internal energy requirements (>30 kcal/mol) inaccessible in this case. Other ions studied include ionized 4-methylpyridine and an isomer. Results obtained for these ions comprise evidence for the structures of odd-electron ionic products of protonated alkyl pyridines and suggest that these ions may have distonic structures.

The dependence of ionic fragmentation on the method of excitation[1] is of considerable interest in tandem mass spectrometry[2,3] since a number of different activation methods are currently used to induce decomposition of mass-selected gas-phase ions. The most commonly used method employs collisions of accelerated ions with neutral target gas (collision-activated dissociation).[2,3] The ion kinetic energies are usually either in the eV range (low-energy collisional activation) or in the keV range (high-energy collisional activation). Low-energy collisional activation is often carried out in quadrupole reaction chambers. This experiment allows optimization of a number of parameters, including the collision energy and the number of activating collisions the ions experience during the reaction time.[2,3] Moreover, comparison of the results obtained under different experimental conditions can yield information concerning the potential energy surfaces and fragmentation dynamics of gas-phase ions, assuming that the effects of the experimental variables are well understood.[2-7]

Our study has a 2-fold goal: (i) to understand better the effects of the various parameters that control collisional activation of ions in quadrupole tandem mass spectrometry, and (ii) to provide further insight into the gas-phase chemistry of some interesting

Scheme I

CONVENTIONAL IONS	DISTONIC IONS
$CH_3OH^{+\cdot}$	$\cdot CH_2OH_2^+$
1	2
$CH_3CH_2OH^{+\cdot}$	$\cdot CH_2CH_2OH_2^+$
3	4
$CH_3CH_2CH_2OH^{+\cdot}$	$\cdot CH_2CH_2CH_2OH_2^+$
5	6
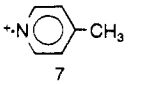	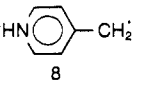
7	8

† National Research Council/Naval Research Laboratory Postdoctoral Research Associate. Present address: Department of Chemistry, Virginia Commonwealth University, Richmond, VA 23284-2006.

0002-7863/90/1512-5110$02.50/0